Title	Farmland Drought Evaluation Based on the Assimilation of Multi-Temporal Multi-Source Remote Sensing Data into AquaCrop Model
Authors(s)	Yang, Guijun; Yang, Hao; Xiuliang, Jin; Silvestro, Paolo Cosmo; et al.
Publication date	2016-07-08
Publication information	Proceedings of Dragon 3 Final Results and Dragon 4 Kick-Off Symposium
Conference details	Dragon 3 Final Results and Dragon 4 Kick-Off Symposium, 4-8 July 2016, Wuhan, China
Publisher	ESA
Item record/more information	http://hdl.handle.net/10197/10201

FARMLAND DROUGHT EVALUATION BASED ON THE ASSIMILATION OF MULTI-TEMPORAL MULTI-SOURCE REMOTE SENSING DATA INTO AQUACROP MODEL

Yang Guijun [(1)], Yang Hao [(1)], Jin Xiuliang [(1)], Pignatti Stefano [(2)], Casa Raffaele [(3)], Silvestro Paolo Cosmo [(3)]

[(1)] *National Engineering Research Center for Information Technology in Agriculture (NERCITA), 2449-26, Beijing 100097, P.R. China, Email: yanggj@nercita.org.cn; yangh@nercita.org.cn*

[(2)] *Consiglio Nazionale delle Ricerche – Institute of Methodologies for Environmental Analysis (C.N.R. – IMAA), Via del Fosso del Cavaliere, 100, 00133 Roma, (Italy) Email: stefano.pignatti@cnr.it*

[(3)] *Università della Tuscia, DAFNE, Via San Camillo de Lellis, 01100, Viterbo (Italy), Email: rcasa@unitus.it; p.c.silvestro@unitus.it*

ABSTRACT

Drought is the most costly natural disasters in China and all over the world. It is very important to evaluate the drought-induced crop yield losses and further improve water use efficiency at regional scale. Firstly, crop biomass was estimated by the combined use of Synthetic Aperture Radar (SAR) and optical remote sensing data. Then the estimated biophysical variable was assimilated into crop growth model (FAO AquaCrop) by the Particle Swarm Optimization (PSO) method from farmland scale to regional scale.

At farmland scale, the most important crop parameters of AquaCrop model were determined to reduce the used parameters in assimilation procedure. The Extended Fourier Amplitude Sensitivity Test (EFAST) method was used for assessing the contribution of different crop parameters to model output. Moreover, the AquaCrop model was calibrated using the experiment data in Xiaotangshan, Beijing.

At regional scale, spatial application of our methods were carried out and validated in the rural area of Yangling, Shaanxi Province, in 2014. This study will provide guideline to make irrigation decision of balancing of water consumption and yield loss.

1. INTRODUCTION

Drought is the most costly natural disasters in China and all over the world. The frequent occurrence of drought, coupled with the impact of global warming, poses an increasingly severe threat to the Chinese agricultural production, especially in semi-arid regions. The grain loss caused by drought accounted for 60% of all grain losses caused by meteorological disasters, resulting in 58% or more of economic losses in China. However, since its definition is spatially variant and context dependent, the accurate and timely drought monitoring and prediction has always been a challenge.

Therefore, in the context of Dragon 3 cooperation project, the main objectives of our project are to develop new methods to monitor and predict farmland drought accurately and timely in agricultural vegetated area basing on multi-source remote sensing data. Our main research work include: *1)* the monitoring of key biophysical variables of crop and soil in farmland drought by optical and radar remote sensing data, *2)* the risk assessment of farmland drought by time series remote sensing and meteorological data, and *3)* the crop loss evaluation under farmland drought mainly based on AquaCrop crop model [1]. In the last 2 years, our cooperation research focused on developing methods for the assimilation of biophysical variables into crop growth model, in order to assess drought-induced crop yield losses at regional scale. The brief description of the work was introduced in the following sections.

2. STUDY AREA AND MATERIALS

2.1 Study Area

The field measurements were conducted in the Yangling district of Shaanxi, China (Figure 1). It is characterized by a typical continental climate and belongs to the semi-arid region of China. The maximum temperature is 26.1°C in the summer, and the minimum temperature is −1.2 °C in the winter. In all the seasons, these climates experience extensive and rapid daily temperature changes, and the temperature difference between day and night is significant. The average annual precipitation is 635.1 mm and the frost-free period is 211 d on average.

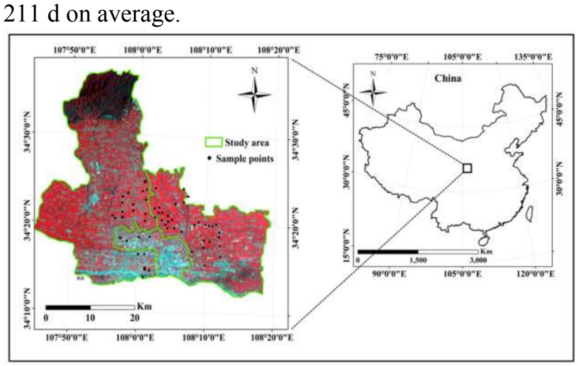

Figure 1. The location map of the study area in Shaanxi, China

2.2 In-situ data and remote sensing data

Field measurements were carried out from March to June for each crop season. The biophysical parameters of crop and soil, including LAI, biomass and soil moisture etc., were measured. Detailed information was presented in [2, 3].

The remote sensing data set consists of several images

Proc. 'Dragon 3 Final Results & Dragon 4 Kick-Off Symposium', Wuhan, PR China, 4–8 July 2016 (ESA SP-739, August 2016)

acquired by Radarsat-2 and HJ 1-A/B during the three crop cycles (Tab. 1).

Table 1. Remote Sensing data set for Yangling

Radarsat-2	HJ 1-A/B
05/03/2014	04/03/2014
29/03/2014	07/04/2014
22/04/2014	29/04/2014
16/05/2014	20/05/2014
09/06/2014	11/06/2014

3. METHODOLOGY

3.1 Biomass estimation from Full Polarization SAR

Two categories of methods were tested: eigenvalue-based and model-based polarimetric scattering decomposition. The Cloude-Pottier method decomposes the coherency matrix into different eigenvectors and eigenvalues which classify and describe the primary scattering mechanisms. Physical information provided by the decomposition is characterized by four variables: entropy (H), alpha angle (α), and anisotropy (A). In contrast, the Freeman-Durden method decomposes the backscatter response into three categories of basic scattering components: volume scattering (Vol), double-bounce scattering (Dbl), and odd scattering (Odd). Typical polarimetric features were utilized for exploring the polarimetric scattering mechanism of oilseed rape. In this research, polarimetric ratios were also constructed based on polarimetric scattering components: Vol/(Odd+Dbl), or Vol/Odd.

The temporal evolution of scattering intensity features and polarimetric features during the entire growing season was analysed as a function of DAS based on all 88 oilseed rape fields. These features will be evaluated to find potential indicators for crop biomass. The evaluation criterion for these indicators is whether the temporal evolution curve is smooth. If the curve is smooth, simple methods can be used to estimate biomass, which will meet the requirements of operational applications.

When just single polarization channel data were available, the three polarization channels, HH, HV, and VV were investigated, respectively. When dual polarization channel data were available, we selected 4 indicators HH/VV, HH/HV, VH/VV (HV $\approx$ VH) and Polarization Discrimination Ratio (PDR). When quad polarization channel data were available, in addition to the decomposition methods described above, we also investigated Radar Vegetation Indices (RVI) as a contrast.

3.2 Biomass estimation by SAR and Optical data

Based on published literature and the sensitivity of optical and polarization features to LAI and biomass, radar polarimetric parameters and optical spectral vegetation indices were used to estimate LAI and biomass of winter wheat in China. In this sub-package, radar polarimetric parameters (HH, HV, VV, HH/VV, HH/HV, VV/HV, Vol/Span, Dbl/Span, Odd/Span, and radar vegetation index (RVI)) and optical vegetation indices (ratio vegetation index (RVI), normalized difference vegetation index (NDVI), soil adjusted vegetation index (SAVI), optimized soil adjusted vegetation index (OSAVI), enhanced vegetation index (EVI), and modified triangular vegetation index (MTVI2)) were selected to analyse the relationships between vegetation indices and LAI, biomass.

Firstly, the relationships of parameters with LAI and biomass were examined using linear and nonlinear regression analysis. The parameters of the satellite images included the optical spectral vegetation indices (OSVIs) of HJ-1A/B and the radar polarimetric parameters (RPPs) of RADARSAT-2. Secondly, LAI and biomass were estimated with combined OSVIs and RPPs (the product of OSVIs and RPPs (COSVI-RPPs)). Finally, the COSVI-RPPs were used to estimate the LAI and biomass with multiple stepwise regression (MSR) and partial least squares regression (PLSR) methods. The MSR combines a forward selection and backward elimination. The PLSR is an extension of the multiple linear regression model (e.g., multiple regression or general stepwise regression).

3.3 AquaCrop model sensitivity analysis

Aquacrop is a "water driven" productivity model that simulates Canopy Cover (CC), biomass and yield of a crop mainly as a function of the water productivity, i.e. the biomass produced per unit of water transpired by the vegetation (Steduto et al. 2009). A more detailed explanation about how the Aquacrop model works is presented by Raes et al. (2009).

The most important crop parameters of AquaCrop model were determined to reduce the used parameters in assimilation procedure. The Extended Fourier Amplitude Sensitivity Test (EFAST) method was used for assessing the contribution of different crop parameters to model output. 40 crop parameters in AquaCrop were selected with fluctuations of $\pm$10%, $\pm$30%, $\pm$50% to evaluate the model output. And in the EFAST method, 2 indicators, including First order sensitivity index (FOSI) and total sensitivity index (TSI), were used to assess the contribution of different crop parameters to 4 model output, including static variables (yield and Maximum dry biomass) and dynamic variables (canopy cover and dry biomass).

3.4 PSO assimilation of AquaCrop model

Particle Sparm Optimization (PSO) method was used in the AquaCrop model assimilation. Firstly, 8 most sensitive model parameters as a particle were selected. Then, we selected the canopy cover or biomass as the data state variables. Run the AquaCrop model in order to obtain an ensemble of N estimated CCs or Biomass. PSO method will update the AquaCrop model to minimum the difference between simulated biomass and remote sensed biomass. Finally we will obtain the yield output. The flowchart of this procedure is showed in

Figure 2.

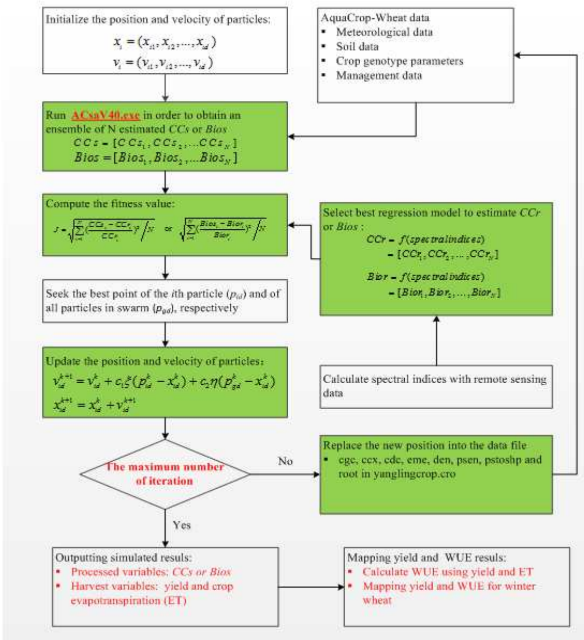

Figure 2. The flowchart of PSO method

4. RESULTS AND DISCUSSION

4.1 Biomass estimation from Full Polarization SAR

The results of the temporal evolution of HH, HV, and VV scattering intensity (in power unit) is presented in Figure 3, which demonstrates their respective scattering response behaviour during the entire growing season [6].

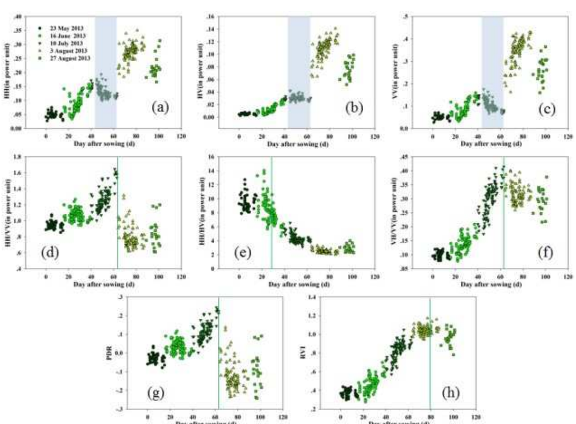

Figure 3. Temporal evolution of different scattering intensity features with DAS. (a)(b)(c), HH, HV, and VV results for single polarization; (d)(e)(f)(g), HH/VV, HH/HV, VH/VV and PDR results for dual polarization; (h) RVI results for quad polarization.

In addition to scattering intensity, unique polarimetric features can be extracted from fully polarimetric SAR data by target polarimetric decomposition methods. In Figure 4, the temporal evolution of Entropy, Alpha, and Anisotropy, 3 classic parameters calculated from the Cloude-Pottier decomposition method are presented.

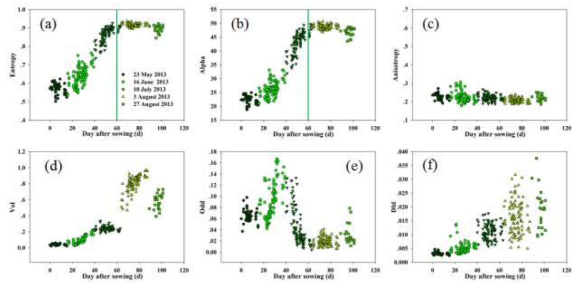

Figure 4 Temporal evolution of different polarimetric features with DAS. (a)(b)(c), Entropy, Alpha, and Anisotropy results by eigenvalue-based decomposition; (d)(e)(f), Volume, Odd, and Double scattering component results by model-based decomposition.

From the Figure 3 and 4, it was revealed that full polarization data have more capability in characterising crop growth, especially when aiming to utilise simple linear models. When we observe the temporal evolution of field observations of biomass and polarimetric ratio, it was found that there is a highly similar pattern between Vol/Odd or Vol/(Odd+Dbl) and biomass parameters when DAS<80. Therefore, it is likely that Vol/Odd or Vol/(Odd+Dbl) have great potential in estimating crop biomass parameters in operational methods.

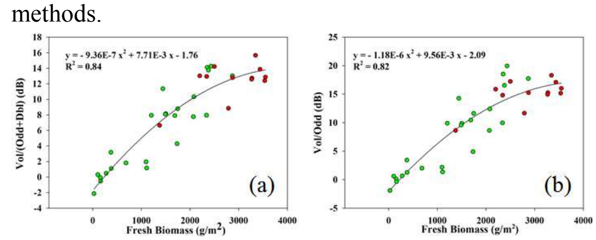

Figure 5 The relationship between fresh biomass and polarimetric indicators, (a) Vol/(Odd+Dbl), (b) Vol/Odd. Red points indicate DAS>75.

4.2 Biomass estimation by SAR and Optical data

Based on the correlations (R^2) between the RPPs and the LAI and biomass from the field experiment, the RPPs that were best correlated with LAI and biomass were RVI (R^2 = 0.63) and DERD (R^2 = 0.71) [3]. Thus, these indices were used to establish the combined optical spectral vegetation indices and radar polarimetric parameters (COSVI-RPPs) by multiplying each with optical spectral vegetation indices (RVI × OSVIs and DERD × OSVIs). In this study, six OSVIs were individually combined with RVI and with DERD to analyze the relationships of these COSVI-RPPs with LAI and biomass. Further, we used these correlations to establish LAI and biomass regression equations for winter wheat. The results revealed the highest R2 value was the MTVI2 × RVI (R2 = 0.68) for winter wheat LAI. In contrast, the highest R2 was the EVI × RVI (R^2

= 0.80) for winter wheat biomass. The results demonstrated that the COSVI-RPPs were highly significantly related to LAI and biomass. They could be used to estimate LAI and biomass in winter wheat.

To validate the estimation accuracy of the regression equations for LAI and biomass, the predicted values and the measured values were compared based on the RMSE and nRMSE. The results was showed in Table 5.6. There was good consistency between the predicted values and the measured values. The RMSE and nRMSE values for the regressions between the MTVI2 × RVI and LAI were 0.65 and 19.52%, and those for the regressions between the EVI × RVI and biomass were 146.33 g/m^2 and 20.21%, respectively. The results showed that MTVI2 × RVI and EVI × RVI were better than RVI, MTVI2 and EVI alone for estimation of LAI and biomass in winter wheat, respectively (Figure 6). The results suggested that the MTVI2 × RVI and EVI × RVI could be used to improve the estimation accuracy of LAI and biomass, respectively.

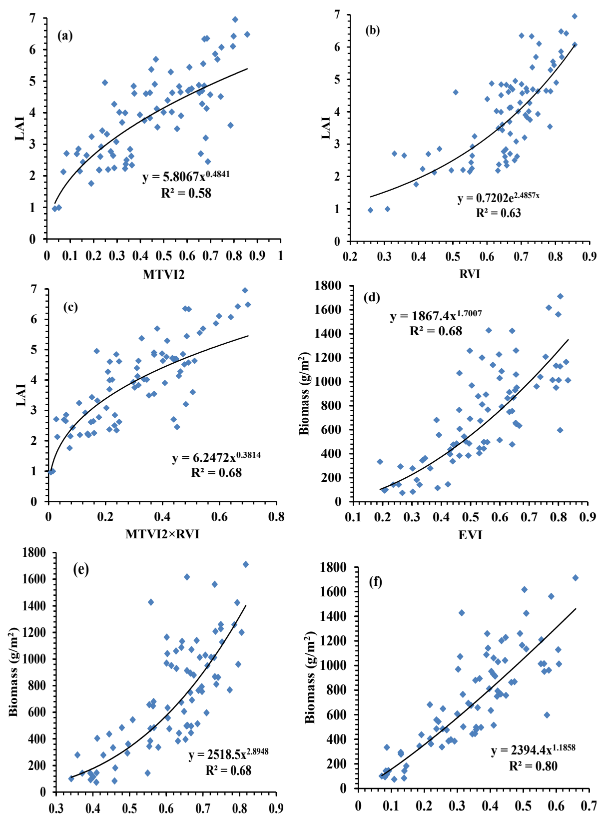

Figure 6. Comparison of MTVI2 (a) RVI (b) and MTVI2×RVI (c) for estimation of LAI and EVI (d), RVI (e) and EVI×RVI (f) for estimation of biomass, respectively.

The MSR and PLSR methods were used to estimate LAI and biomass for winter wheat based on the combined, optical and radar indices. The LAI values were estimated from MSR and PLSR regression equations obtained based on all the combined optical and polarimetric radar indices, which had R^2 values of 0.73 and 0.76, respectively. Similarly, the biomass values were estimated from MSR and PLSR regression equations and the R^2 values were 0.81 and 0.85, respectively (Table 2). All the COSVI-RPPs, OSVIs, and RPPs were selected as variables to estimate LAI using MSR and PLSR, and the R^2 values of the regression equation were 0.74 and 0.78, respectively. The R^2 of the MSR and PLSR biomass models based on all the COSVI-RPPs, OSVIs, and RPPs were 0.83 and 0.87, respectively.

Table 2 Comparison of multiple stepwise regression and partial least squares regression methods for estimating LAI and biomass of winter wheat based on OSVIs, RPPs, and COSVI-RPPs (n = 80)

Methods	Variables	R^2	RMSE (g/m^2)	nRMSE (%)
Multiple Stepwise regression	SAVI × RVI, OSAVI × DERD, MTVI2 × DERD	0.81**	142.63	19.71
Partial least squares regression	12 COSVI-RPPs	0.85**	137.21	18.96
Multiple stepwise regression	MTVI2, DERD, SAVI × RVI, OSAVI × DERD, MTVI2 × DERD,	0.83**	140.34	19.39
Partial least squares regression	12 COSVI-RPPs, 6 OSVIs, 15 RPPs	0.87**	134.68	18.61

4.3 AquaCrop model sensitivity analysis

Figure 7 showed the sensitivity analysis results of AquaCrop model by EFAST method. The Figure 7(a) was the first order sensitivity index (FOSI) result for yield. And Figure 7 (b) is the total sensitivity index (TSI) result for yield. The Figure 8 is the FOSI results for time series dry biomass under different parameter variation ranges.

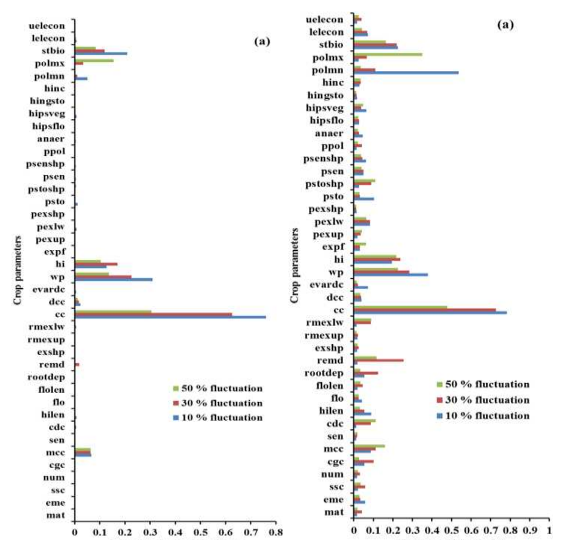

Figure 7. Sensitivity analysis results (a) FOSI result for

yield (b) TSI result for yield.

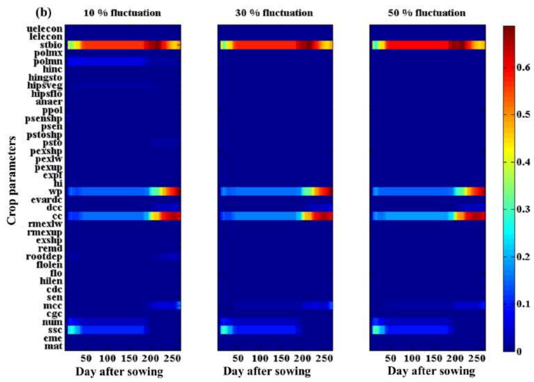

Figure 8. FOSI results for time series dry biomass under different parameter variation ranges

4.4 PSO assimilation of AquaCrop model

Based on the PSO method, the crop biomass was predicted by the combination of AquaCrop model and remote sensing data. Figure 9 presented the biomass result for winter wheat in Yangling district. It shows good consistency between the predicted and the measured for canopy cover and Biomass.

When the biomass was as dynamic variables to apply the data assimilation, Figure 10 presented the relationship between predicted and measured yield for winter wheat in Yangling district.

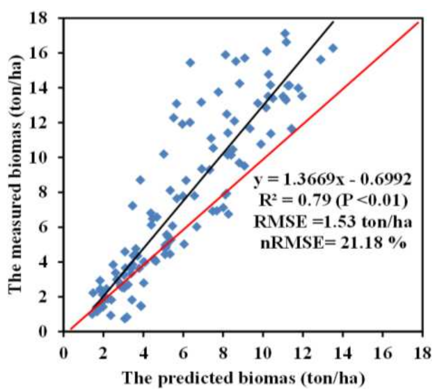

Figure 9. Relationships between predicted and measured biomass for winter wheat in Yangling district

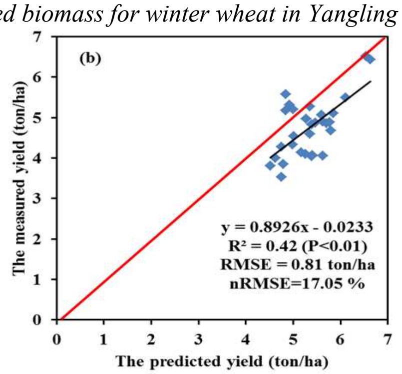

Figure10. Relationship between predicted and measured yield for winter wheat

Figure 11 presented the winter wheat yield mapping in Yangling by PSO method when the biomass as the dynamic variable was inputted into apply the processing of assimilation method. The result revealed that the predict grain yeild was very in agreement with the measured GY (R^2 = 0.42 and RMSE =0.81 ton/ha).

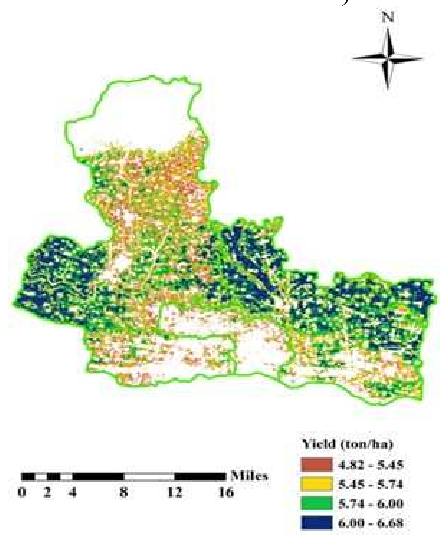

Figure 11. Yield mapping in Yangling by PSO method

5. CONCLUSION

- PSO method which assimilates the remote sensing observation and AquaCrop model can be used to estimate the yield and WUE at regional scale;
- Biomass is more suitable than CC as a state variable in PSO assimilation; and the estimation result of yield based on Biomass (R^2=0.42, RMSE = 0.81ton/ha, nRMSE = 17.05%) is better than that based on CC (R^2 = 0.31, RMSE = 0.94ton/ha and nRMSE = 19.79%);
- This study provide a method for monitoring the yield and WUE in regional scale by combining the AquaCrop model and RS observation;
- This study provide a guideline for improving the irrigation management of winter wheat in arid regions.

6. REFERENCES

1. Yang, G., Yang, H., Jin, X., Pignatti S., Casa R., Pascucci S., Silverstro P.C. (2014) Research progress of farmland drought monitoring and prediction based on multi-source remote sensing data. ESA SP-724, ESA Publications Division, European Space Agency.

2. Silvestro, P.C., Casa, R., Pignatti, S., Castaldi, F., Yang, H. & Yang, G. (2016). Assimilation of remotely sensed data into crop models for farmland drought assessment: a comparison of models of differing complexity. In '2016 Dragon 3 final results Symposium, Wuhan, China', ESA Publications Division, European Space Agency.

3. Jin, X., Yang, G., Xu, X., Yang, H., Feng, H., Li, Z., Shen, J., Zhao, C., & Lan, Y. (2015). Combined Multi-Temporal Optical and Radar Parameters for Estimating LAI and Biomass in Winter Wheat Using HJ and RADARSAR-2 Data. *Remote Sensing*, 7(10), 13251-13272.

4. Yang, H., Li, Z., Chen, E., Zhao, C., Yang, G., Casa, R., Pignatti, S., & Feng, Q. (2014). Temporal Polarimetric Behavior of Oilseed Rape (Brassica napus L.) at C-Band for Early Season Sowing Date Monitoring. *Remote sensing*, 6(11):10375-10394.

5. Yang, H., Chen, E., Li, Z., Zhao, C., Yang, G., Pignatti, S., Casa, R., & Zhao, L. (2015). Wheat lodging monitoring using polarimetric index from RADARSAT-2 data. *International Journal of Applied Earth Observation and Geoinformation*, 34, 157-166.

6. Yang, H., Yang, G., Gaulton, R., Zhao, C., Li, Z., Taylor, J., Wicks, D., Minchella, A., Chen, E., Yang, X. In-season Biomass Estimation of Oilseed Rape (*Brassica napus L.*) Using Fully Polarimtric SAR Imagery. *Precision Agriculture*. (in review)

7. Jin, X., Feng, H., Zhu, X., Li, Z., Song, S., Song, X., Yang, G., Xu, X. & Guo, W. (2014). Assessment of the AquaCrop Model for Use in Simulation of Irrigated Winter Wheat Canopy Cover, Biomass, and Grain Yield in the North China Plain. PLoS ONE , 9(1): 1–11.

8. Silvestro, P.C., Casa, R., Pignatti, S., Castaldi, F., Yang, H. & Yang, G. (2014). Development of an Assimilation Scheme for the Estimation of Drought-Induced Yield Losses Based on Multi-Source Remote Sensing and the Acquacrop Model. In '2014 Dragon 3 mid-term results Symposium, Chengdu, China', ESA SP-724, ESA Publications Division, European Space Agency.